Desalination 422 (2017) 182–193

Contents lists available at ScienceDirect

Desalination

journal homepage: www.elsevier.com/locate/desal

Cost-based feasibility study and sensitivity analysis of a new draw solution assisted reverse osmosis (DSARO) process for seawater desalination

Kiho Park, Do Yeon Kim, Dae Ryook Yang*

Department of Chemical and Biological Engineering, Korea University, Seoul, Republic of Korea

GRAPHICAL ABSTRACT

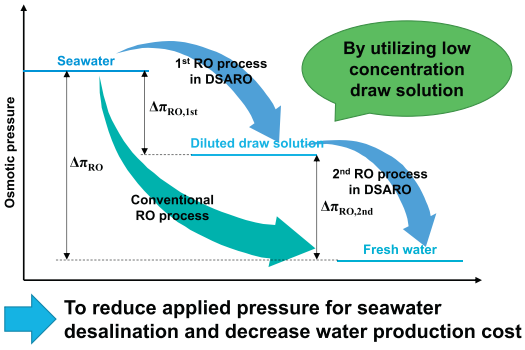

ARTICLE INFO

Keywords:
Draw solution assisted reverse osmosis
Modeling
Seawater desalination
Process design
Draw solution
Cost estimation
Reverse osmosis

ABSTRACT

In this study, a newly devised seawater desalination process, namely, the draw solution assisted reverse osmosis (DSARO) process, is proposed. A mathematical model for the DSARO process was developed and energy consumption and economic evaluation models were constructed to assess the feasibility of the DSARO process compared to the conventional reverse osmosis (RO) process. This work presents a characterization of important variables and the research on the effects of these variables. Compared to the conventional RO process, the DSARO process could have a 10% lower specific water production cost. The operating pressures required to reach 40% of overall recovery were approximately 35 bar in the 1st RO process, and 30 bar in the 2nd RO process. Due to its operating pressure being lower than the conventional RO process, the capital and membrane replacement costs could be reduced. The required conditions in the 1st RO membrane to drive the DSARO process were that the membrane structure parameter must be lower than 0.13 mm, and the maximum operating pressure should be higher than 35 bar. Even though these conditions are not available commercially at present, they could be attained based on the best available membrane technology in the literature.

1. Introduction

Until now, forward osmosis (FO) has attracted many researchers to investigate and analyze the potential of the FO process as an alternative to the reverse osmosis (RO) process for seawater desalination [1–3]. Even though its characteristic of spontaneous water transport from seawater to draw solution by osmotic pressure difference appears very energy-efficient, the overall energy-efficiency in the system containing draw solution recovery units cannot easily be lower than the RO system. That is because the theoretical minimum energy demand to separate fresh water from the draw solution in the FO process is eventually higher than when separating water from the seawater

* Corresponding author.
E-mail address: dryang@korea.ac.kr (D.R. Yang).

http://dx.doi.org/10.1016/j.desal.2017.08.026
Received 31 May 2017; Received in revised form 17 August 2017; Accepted 24 August 2017

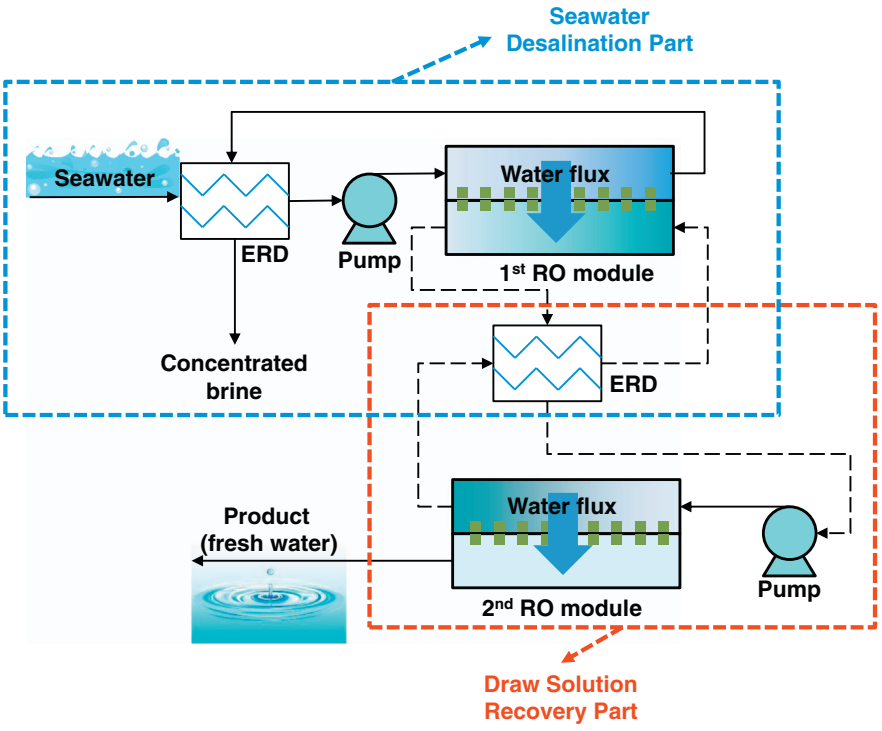

Fig. 1. Schematic diagram of the DSARO process.

directly in the RO process [4,5]. In other words, the draw solution recovery process in the FO system needs to be more energy-efficient than the RO process to secure a competitiveness of the FO system as an alternative process for seawater desalination. In addition, the FO system for seawater desalination is a two-stage process, first seawater desalination by the FO process, and then draw solution recovery by other separation processes, such as RO or membrane distillation (MD) [6]. Since this two-stage process requires more equipment than a single-stage process, the initial capital cost of the FO system could be higher than the RO system. Thus, it is not easy for a stand-alone FO system to be utilized as an alternative process for seawater desalination.

However, the concept of the FO process is still useful, and many applications have been investigated to utilize the concept of FO process efficiently [1,4,5,7–9]. There are two FO applications: 1) seawater desalination by hybridization with the other technologies, and 2) wastewater treatment and reclamation. The former includes an indirect desalination FO system with an RO process [10–12], FO-crystallization-RO hybrid process [13], FO-electrodialysis-RO hybrid process [14], and FO with renewable energy [15,16]. Especially, FO coupled with thermal separation process can utilize low-grade thermal energy which cannot be an energy source in the conventional RO process, and enables to separate highly saline water which cannot be usually treated by the conventional RO process due to the pressure limitation [5,17]. Compared to the conventional thermal process for desalination, e.g. multi-staged flash (MSF), the FO coupled with thermal separation process can reduce operating cost, power consumption, and fouling propensity [17]. The latter comprises oily wastewater treatment [7,18], heavy metal removal [19], and water reclamation with fertilizer as draw solution [20]. In the last case, the draw solution recovery process is unnecessary since the draw solution could be directly utilized as fertilizer. Therefore, the concept of an osmotically driven process by draw solution can still be widely applied in various fields and applications.

The main obstacle of the seawater desalination process is its high osmotic pressure (around 26 bar for 35 g/l seawater) [9]. In other words, if the osmotic pressure in seawater could be reduced, the energy consumption and water production cost in the seawater desalination process could decrease significantly. In the conventional FO process, the concentration of the draw solution is usually higher than that of seawater so as to drive the FO process spontaneously by the osmotic pressure difference. However, if the concentration of draw solution was slightly lower than the seawater's, and the low concentration draw solution was located on the draw solution side in the FO module with the seawater on the feed solution side, the osmotic pressure difference between these solutions would decrease significantly [21,22]. In this case, water permeation could occur by applying a light pressure on the feed solution. Therefore, a lower osmotic pressure difference requires a lower operating pressure for an RO system. If the salt concentration of seawater cannot be lowered, the relative osmotic pressure difference can be lowered by applying a solution that has a higher concentration than pure water, but lower than that of seawater. In other words, this idea is a utilization of the concept of draw solution using different method, not inducing spontaneous water molecules transfer, but decreasing the osmotic pressure difference. In this case, the RO module has to be modified in a similar way to the pressure retarded osmosis (PRO) module as the RO module must withstand a relatively high pressure, and both solutions should be located across a semi-permeable membrane.

In this study, a new desalination method, named draw solution assisted reverse osmosis (DSARO) is proposed. In this process, a draw solution, whose concentration is lower than that of seawater, was utilized to reduce the osmotic pressure difference between the seawater and the draw solution. Thus, an operating pressure lower than that of the conventional RO process would be required to drive the DSARO process. A mathematical model to describe the DSARO process was developed and energy consumption and cost estimation models were developed to assess the economic feasibility of the process, as compared to the conventional RO process. Through a sensitivity analysis, a detailed analysis was presented on cost ratios to calculate the DSARO process from the desalination plant cost data. Finally, the required conditions to realize the DSARO process were suggested, and the feasibility of the DSARO process with the best available membrane technology at the present time was discussed.

2. Methods

2.1. Description of the DSARO process

A schematic diagram of the DSARO process is shown in Fig. 1. The process has two parts: seawater desalination from the 1st RO module, and draw solution recovery from the 2nd RO module. First, a seawater feed stream, which is assumed to be pre-treated seawater, is fed into the feed side of the 1st RO module. The draw solution, whose concentration is lower than that of seawater, is then placed on the draw side of the 1st RO module. The draw solute is assumed to be sodium chloride in this study. As the feed stream is pressurized by the high-pressure pump before the 1st RO module, water molecules in the seawater feed stream are permeated into the draw side of the 1st RO module. Since the osmotic pressure difference between the seawater and the draw solution is significantly lower than the osmotic pressure of the seawater itself, the pressure requirement to drive the 1st RO process could be reduced compared to the conventional RO process. The pressurized feed retentate stream from the 1st RO module is fed into an energy recovery device (ERD) to reclaim the pressure energy of the retentate feed stream. After the ERD, the retentate feed stream is disposed of. The draw solution is diluted through the 1st RO module due to the permeate water flux. The diluted draw solution is then pumped and flows into the 2nd RO module to produce fresh water. The retentate stream from the 2nd RO module, which is the concentrated draw solution from the 2nd RO module, is sent to a 2nd ERD for pressure recovery, and recycled into the 1st RO module as the draw solution feed stream. With this procedure, the overall process is established and the draw solution recycle stream is completed.

The most remarkable feature of the DSARO process is that it can change the high-pressure single-stage RO process to a low-pressure two-stage process with assistance of the low concentration draw solution as shown in Fig. 2. Therefore, it can obviate the need for equipment that can withstand high-pressure operation, so the capital cost of the DSARO process can be reduced compared to that of the conventional RO process. In addition, high irreversible fouling propensity, which is the main reason of membrane replacement costs, can be significantly alleviated. So, it can reduce the operating costs of the DSARO process. Compared to the FO process, the DSARO process would not increase the theoretical minimum energy requirement as shown in Fig. 2. From these features, the DSARO process could have a potential to become a low-cost seawater desalination process compared to the conventional RO process. To assess the feasibility of the DSARO process as an alternative, a mathematical model to describe the process should be developed, and a cost-based analysis based on the model should also be performed with the conventional RO process under same basis.

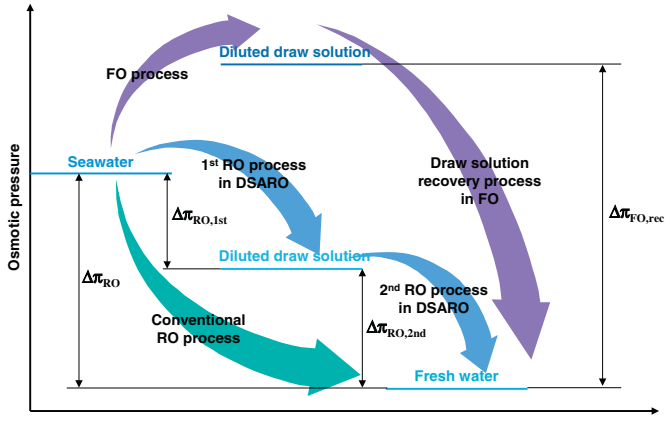

Fig. 2. Illustration of theoretical osmotic pressure difference in the conventional RO, DSARO, and FO processes.

2.2. Mathematical modeling

2.2.1. Flux equations

The 1st RO process is similar to the FO process, and the 2nd RO process is the same as the brackish water reverse osmosis (BWRO) process. Thus, the flux equations in the DSARO process can be taken from the generalized flux equations usually employed in the FO and RO processes, expressed as [23–25]

$$J_w = A(\Delta P - \Delta\pi) \tag{1}$$

$$J_s = B(C_D - C_F) \tag{2}$$

where J_w is the water flux, J_s is the salt flux, A is the water permeability, B is the salt permeability, $\Delta\pi$ is the osmotic pressure difference, ΔP is the applied pressure in the RO module, C is the concentration, and subscripts D and F are the draw solution and feed solution, respectively.

The osmotic pressures in the draw and feed solutions were estimated from the van't Hoff equation:

$$\pi = \frac{N_{ion} CRT}{M_w} \tag{3}$$

where, R is the gas constant, T is the temperature, N_{ion} is the ionization number, and M_w is the molecular weight.

2.2.2. External concentration polarization (ECP)

External concentration polarization (ECP) took place in the 1st and 2nd RO processes due to water permeate flux in each process. It can be expressed using the boundary layer film theory with mass transfer coefficient as [23,26]:

$$\frac{\pi_{F,m}}{\pi_{F,b}} = \exp\left(\frac{J_w}{k}\right) \quad \text{(AL-FS mode)} \tag{4}$$

$$\frac{\pi_{D,m}}{\pi_{D,b}} = \exp\left(-\frac{J_w}{k}\right) \quad \text{(AL-DS mode)} \tag{5}$$

$$k = \frac{Sh \cdot D}{d_h} \tag{6}$$

$$Sh = 1.85\left(Re\, Sc \frac{d_h}{L}\right)^{0.33} \quad \text{(laminar flow)} \tag{7}$$

$$Sh = 0.04 Re^{0.75} Sc^{0.33} \quad \text{(turbulent flow)} \tag{8}$$

where k is the mass transfer coefficient, Sh is the Sherwood number, D is the diffusivity, d_h is the hydraulic diameter, Re is the Reynolds number, Sc is the Schmidt number, L is the channel length, and subscripts m and b are the membrane surface and the bulk solution, respectively.

2.2.3. Internal concentration polarization (ICP)

Since the water flux changes the solution concentrations at the surface of the membrane, and the porous structure of the membrane support layer hinders solute molecules from migrating freely within the support layer, internal concentration polarization appears in the porous support layer of the membrane as in the conventional FO process. However, as shown in Fig. 3, the shape of the internal concentration polarization (ICP) is quite different to the FO process, as the direction of the water flux is opposite to that of the FO process. Nevertheless, the ICP appearance negatively influences the energy consumption in the 1st RO module, as the increased effective osmotic pressure difference demands a higher applied pressure to produce water flux. Thus, the ICP effect should be considered to correctly estimate energy consumption in the DSARO process.

The ICP model was developed based on the solution-diffusion theory. Assuming that salt rejection in the porous support layer consists of two components, diffusion and convection terms, the ICP model can be derived as [22,27,28]:

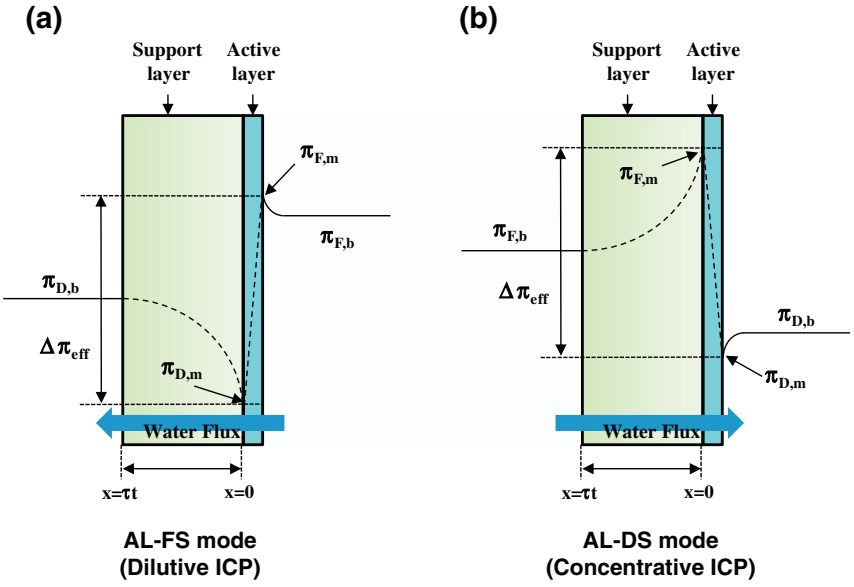

Fig. 3. Concentration polarization in the DSARO process: (a) active layer-feed solution mode (AL-FS mode), and (b) active layer-draw solution mode (AL-DS mode).

$$\underbrace{B(C_{F,m}-C_{D,m})}_{\text{Salt flux}}-\underbrace{D\varepsilon\frac{dC(x)}{dx}}_{\text{Diffusive flux}}+\underbrace{J_wC(x)}_{\text{Convective flux}}=0 \tag{9}$$

Boundary conditions for the 1st RO process are:

$$\begin{bmatrix}C(x)=C_{D,m}\text{ at }x=0\\C(x)=C_{D,b}\text{ at }x=\tau t\end{bmatrix}\quad\text{at AL-FS} \tag{10}$$

$$\begin{bmatrix}C(x)=C_{F,m}\text{ at }x=0\\C(x)=C_{F,b}\text{ at }x=\tau t\end{bmatrix}\quad\text{at AL-DS} \tag{11}$$

where t is the thickness, τ is the tortuosity, and ε is the porosity of the porous support layer. With these boundary conditions, Eq. (9) can be solved to obtain equations that describe concentrations at the surface of the membrane:

$$C_{D,m}=C_{F,\mathrm{m}}-\frac{C_{F,m}-C_{D,b}\exp(-J_wK)}{1+\frac{B}{J_w}(\exp(-J_wK)-1)}\quad\text{at AL-FS} \tag{12}$$

$$C_{F,m}=C_{D,\mathrm{m}}-\frac{C_{D,m}-C_{F,b}\exp(J_wK)}{1-\frac{B}{J_w}(\exp(J_wK)-1)}\quad\text{at AL-DS} \tag{13}$$

$$K=\frac{\tau t}{D\varepsilon}=\frac{S}{D} \tag{14}$$

After calculating the ECP at the surface of the active layer from Eqs. (4) and (5), the effect of ICP can be determined from the membrane characteristics, salt diffusivity, salt permeability, and water flux. Since the concentrations at the surface of the membrane are required to calculate the water flux as seen in Eq. (1), the model's equations are implicitly coupled. Thus, it should be carefully solved iteratively and numerically.

2.2.4. Mass and momentum balance equations

The mass and momentum balance equations along the membrane length are described with assumptions that the temperature dependency of density, the volume of solute in the solution, and the solute diffusion in an axial direction can be neglected [24,29,30]:

[Feed side, 1st RO module]

$$\frac{du_F}{dx}=-\frac{J_w}{H}$$
$$\frac{dC_F}{dx}=\frac{-J_s+C_FJ_w}{u_FH}$$
$$\frac{dP_F}{dx}=\frac{-k_{fric}\mu_Fu_F}{H^2} \tag{15}$$

[Draw side, 1st RO module]

$$\frac{du_D}{dx}=\frac{J_w}{H}$$
$$\frac{dC_D}{dx}=\frac{J_s-C_DJ_w}{u_DH}$$
$$\frac{dP_D}{dx}=\frac{-k_{fric}\mu_Du_D}{H^2} \tag{16}$$

[Feed side, 2nd RO module]

$$\frac{du}{dx}=-\frac{J_w}{H}$$
$$\frac{dC}{dx}=\frac{-J_s+CJ_w}{uH}$$
$$\frac{dP}{dx}=\frac{-k_{fric}\mu u}{H^2} \tag{17}$$

where, u is the linear velocity, k_{fric} is the friction coefficient, μ is the viscosity, and H is the channel height. The flow direction in the 1st RO module was assumed as counter-current. Thus, a shooting method was employed to simulate counter-current flow in the 1st RO module.

2.3. Energy consumption model

In the DSARO process, most of the energy is required to drive pumps. As shown in Fig. 4, there are several pumps required to operate the DSARO process: the seawater intake pump, high-pressure pump, booster pump, and the draw solution circulating pump. In this study, it is assumed that all of the pumps have same efficiency, and friction losses through pipelines are negligible. The energy consumption of the pumps can be calculated from the pressure requirements and flow rates of the inlet streams to each pump.

In the 1st RO process, four different pumps are required to drive the process. The energy consumption for each pump can be given as [31,32]:

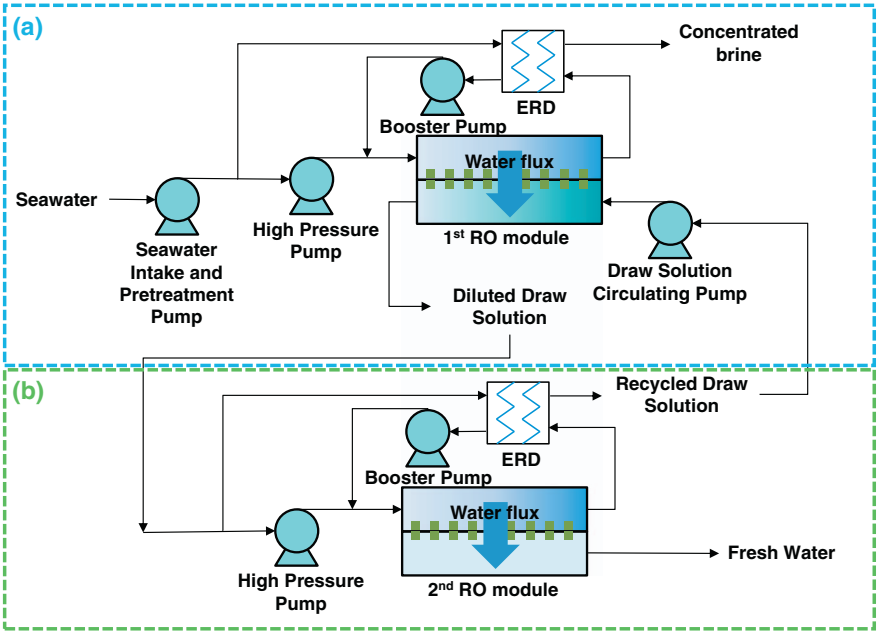

Fig. 4. Detailed schematic diagram of the DSARO process showing pump requirements in each flow stream: (a) 1st RO process, and (b) 2nd RO process.

$$E_{SWIP} = \frac{P_{SWIP} F_F}{\eta_{pump}} \tag{18}$$

$$E_{HPP} = \frac{(F_F - F_{reten})}{\eta_{pump}} (P_F - P_0) \tag{19}$$

$$E_{BP} = \frac{F_{reten}}{\eta_{pump}} (P_F - P_{ERD}) \tag{20}$$

$$E_{DSCP} = \frac{F_D \Delta P_{RO,1st}}{\eta_{pump}} \tag{21}$$

where, P_{SWIP} is the pressure requirement in the seawater intake pump, η_{pump} is the pump efficiency, F is the volumetric flow rate, P_0 is the ambient pressure, P_{ERD} is the pressure of the feed stream after ERD, $\Delta P_{RO,1st}$ is the pressure drop in the 1st RO module, and subscript *reten* is the retentate stream of seawater feed after the 1st RO module. The $\Delta P_{RO,1st}$ can be calculated from the balance equations in section 2.2.4. The P_{ERD} was estimated by [13]:

$$P_{ERD} = \eta_{ERD}(1 - r_{RO,1st})(P_F - \Delta P_{RO,1st} - P_0) + P_0 \tag{22}$$

where, η_{ERD} is the ERD efficiency and $r_{RO,1st}$ is the recovery of the 1st RO module.

In the 2nd RO process, the energy calculation method is the same as that of the 1st RO process except the fact that the seawater intake pump and draw solution circulating pump are not included in the 2nd RO process. Thus, Eqs. (19) and (20) can be employed to estimate the energy consumption in the 2nd RO process.

The specific energy consumption (SEC) in the DSARO process can now be calculated by using:

$$\text{SEC} = \frac{(E_{SWIP} + E_{HPP} + E_{BP} + E_{DSCP})_{1st.RO}}{F_p} + \frac{(E_{HPP} + E_{BP})_{2nd.RO}}{F_p} \tag{23}$$

where F_p is the water production rate.

2.4. Cost estimation model

A cost estimation model is required to assess the feasibility of a new process by comparing water production costs of the new process with that of a conventional process. The model usually comprises capital expenditure (CAPEX) and operating expenditure (OPEX) [33]. CAPEX includes the installation costs of process equipment, construction, engineering, procurement, and contingency costs at the start of plant construction. OPEX is operating and maintenance costs for continuous and sustainable operation of the plant.

CAPEX can be divided into direct and indirect capital costs. The direct capital cost is usually estimated from cost data collected from already-constructed desalination plants worldwide. To calculate the engineering-procurement construction (EPC) cost for an RO plant, which is considered to be a direct capital cost, a statistical model was employed in this study [34].

$$\ln(EPC) = 58.054 + 0.939 \times \ln(CAP) - 0.028 \times YEAR + 0.830 \times TYPE - 0.074 \times REGION \tag{24}$$

where, *CAP* is the capacity of the RO plant, *YEAR* is the construction year, *TYPE* is the type of the RO plant, *TYPE* = 1 and 0 for seawater reverse osmosis (SWRO) and BWRO, respectively, and *REGION* is where the plant is located, *REGION* = 1 and 0 for Gulf Cooperation Council and southern European countries, respectively. The indirect capital cost was estimated as a function of direct capital cost as shown in Table 1 [35,36].

The OPEX includes the cost of electricity, membrane replacement, labor, spares, and chemical treatment [35,36]. The mathematical models described above were utilized to estimate the electricity consumption in the conventional RO and DSARO processes. The cost of electricity can then be estimated as:

$$OC_{elec} = [E_{SWIP} + E_{HPP} + E_{BP} + E_{DSCP}] \times D_{energy} \times L_f \tag{25}$$

where, D_{energy} is the electricity unit cost, and L_f is the plant load factor. The membrane replacement cost is changed according to the applied pressure, as high applied pressure leads to more irreversible fouling. Thus, the membrane replacement cost can be estimated from the capital cost of membranes [32,37,38]

$$OC_{memb.re} = 0.2 \times CC_{memb} \quad \text{[SWRO module]} \tag{26}$$

$$OC_{memb.re} = 0.1 \times CC_{memb} \quad \text{[BWRO module]} \tag{27}$$

where CC_{memb} is the capital cost of membrane. The CC_{memb} can be estimated as a percentage of the total direct capital cost. According to [39], the capital cost of membranes was estimated at approximately 14% of the total direct capital cost. The spare parts replacement and insurance cost for sustainable operation, chemical cost of product

Table 1
Cost estimation model equations in this study.

	Cost functions	Reference
CAPEX		
Direct capital cost		
EPC cost	Eq. (24)	[34]
Indirect capital cost		
Freight & insurance rate during construction	5% of direct capital cost	[35,36]
Owner's cost rate	7.6% of direct capital cost	[35,36]
Contingency rate	10% of direct capital cost	[35,36]
Construction overhead	12.24% of direct capital cost	[35,36]
OPEX		
Cost of electricity	Eq. (25)	[31,32]
Membrane replacement cost	Eqns. (26) and (27)	[32,37,38]
Spare parts replacement and insurance cost	Eq. (28)	[36]
Chemical cost of product water	Eq. (29)	[35,36]
Labor cost	Eq. (30)	[35,36]

water, and labor cost were obtained from [35,36,40]:

$$OC_{spare} = 0.02 \times \text{direct capital cost} \quad (28)$$

$$OC_{chem} = 0.025 \times F_p \times L_f \quad (29)$$

$$OC_{labor} = 0.05 \times F_p \times L_f \quad (30)$$

The total annualized cost (TAC) was calculated as the sum of the total annualized capital cost (TACC) and OPEX. The TACC can be calculated by using an amortization factor, which determines the TACC from CAPEX by taking into account the plant lifespan and interest rate [32].

$$\text{TAC} = \frac{i(i+1)^n}{(i+1)^n - 1} \times \text{CAPEX} + (OC_{elec} + OC_{memb,re} + OC_{spare} + OC_{chem} + OC_{labor}) \quad (31)$$

Finally, specific water production cost (SWC) was calculated by:

$$\text{SWC} = \frac{\text{TAC}}{F_p \times L_f} \quad (32)$$

The parameters used in the cost and energy consumption estimation models are summarized in Table 2.

2.5. Important variable/parameter selection

There are many variables and parameters in the DSARO process; therefore, they should be classified according to their influences on the process in order to simplify the analysis and discussion. Some variables are dependent on other variables, and some variables should be fixed to simplify the energy and cost analysis. In this section, variables and parameters are classified according to their nature, and the important variables and parameters are identified. The remaining variables were either fixed or their relationship with independent variables was defined.

Table 2
Parameters of the cost and energy consumption estimation models.

Parameter	Value	Reference
Feed salinity	35,000 (ppm)	
Pump efficiency (η_{pump})	85 (%)	[41,42]
ERD efficiency (η_{ERD})	95 (%)	[41,42]
Electricity unit cost (D_{energy})	0.08 ($/kWh)	[43]
Plant load factor (L_f)	0.9 (−)	[32]
Intake pump pressure (P_{SWIP})	5 (bar)	[31]
Plant life (n)	20 (year)	[36]
Interest rate (i)	0.06 (1/year)	[11]
Water production rate (F_p)	3,650,000 (m^3/year)	
Construction year (*YEAR*)	2017 (year)	
Plant located region (*REGION*)	0 (southern European countries)	

Table 3
Variables/parameters classification list.

Equipment parameters	System design variables	Operation variables
Pump efficiency	Feed salinity	Feed flow rate
ERD efficiency	Water production rate	Draw flow rate
Intake pump pressure	Plant life	Draw concentration
Water permeability	Plant located region	1st RO applied pressure
Salt permeability	Electricity unit cost	2nd RO applied pressure
Structure parameter	Plant load factor	1st RO recovery
Membrane active area	Interest rate	2nd RO recovery
	Construction year	
	Number of membrane modules (series)	
	Number of membrane modules (parallel)	

2.5.1. Variable/parameter classification

As shown in Table 3, the variables and parameters are classified into three groups; first, equipment parameters which are determined according to characteristics of each equipment, second, system design variables which are fixed at the stage of plant construction, and third, operation variables which can be changed in operation.

2.5.2. Important variables and parameters

The important and independent variables in the DSARO process are the concentration of draw solution (C_{draw}), volumetric flow rate ratio in the 1st RO process (Q_{draw}/Q_{feed}), and membrane structure parameter (S). The C_{draw} can change the osmotic pressure difference, so the energy consumption of the DSARO process can be significantly changed by the C_{draw}. With a fixed recovery ratio of the 1st RO, rec_{1st}, the effluent stream concentration of the draw solution can be varied by Q_{draw}/Q_{feed}. The Q_{draw} would change the pumping energy in the 2nd RO process, which is why Q_{draw}/Q_{feed} was selected as an important variable. Finally, the degree of ICP is directly affected by the S parameter. As the ICP influences the increment of the effective osmotic pressure difference, the S parameter is important in determining the applied pressure in the 1st RO process.

2.5.3. Fixed variables and parameters

To simplify the analysis of the DSARO process in this study, some variables and parameters, which are less important, should be fixed. For this study, the numbers of series module arrangement in the 1st and 2nd RO processes (N_{s_1st}, N_{s_2nd}), the numbers of parallel module arrangement in the 1st and 2nd RO processes (N_{p_1st}, N_{p_2nd}), feed linear velocities in each process (u_F, u), water permeabilities of the membranes (A_{1st}, A_{2nd}), salt permeabilities of the membranes (B_{1st}, B_{2nd}), and the recovery of the 1st RO module (rec_{1st}), were fixed based on references. Since these variables and parameters are generally correlated with the capital cost estimation of the process that was already conducted based on the plant cost data, they can be fixed as normal operating data in the conventional RO process. The rec_{1st} and the numbers of series module arrangement in a single pressure vessel were assumed as 40–45% and 5–7, respectively [44], and, the membrane module was assumed to be an 8-in spiral-wound type. The water and salt permeabilities in the SWRO and BWRO modules, made by Dow Chemical, were employed in this study [45], and these values were selected according to the applied pressure conditions. The u_F and u were fixed at 0.15 m/s to keep the feed flow rate within the flow-rate range specification provided by the membrane module manufacturer [46].

Finally, N_{p_1st}, N_{p_2nd} were determined to satisfy the target water production rate.

The dependent variables, which are automatically determined if all of the independent variables are fixed, were the recovery of the 2nd RO process (rec_{2nd}), applied pressure in the 1st RO module (ΔP_{1st}), and applied pressure in the 2nd RO module (ΔP_{2nd}). The rec_{2nd} is determined under the assumption that the amount of water recovered in the 1st RO module should be recovered in the 2nd RO module to complete the recycle stream of draw solution. After rec_{1st} and rec_{2nd} were fixed, the applied pressures in each process could be obtained if the number of series arrangements in each module, volumetric flow rate, and water permeability of the membrane were determined.

3. Results and discussion

3.1. Effect of concentration polarization with different draw concentrations and structure parameter

As described in Section 2, concentration polarization negatively affects the applied pressure by increasing the effective osmotic pressure difference. The bulk and effective osmotic pressure differences with changing draw solution concentrations and membrane structure parameters in the 1st RO module are shown in Fig. 5. The applied pressure in this simulation was fixed at 40 bar. The effective osmotic pressure difference increases significantly as the membrane structure parameter increases. Even though the bulk osmotic pressure difference is very low at 30 g/l of draw solution concentration, a large ICP effect would make the draw solution ineffective. Thus, the concentration polarization effect should be minimized to utilize the concept of the DSARO process efficiently. The simulation results also revealed that the membrane orientation in the AL-FS mode is more efficient in terms of concentration polarization than the AL-DS mode, due to a lower concentration polarization in the AL-FS mode. The AL-FS mode is usually applied in the seawater desalination process as, if the porous support layer is located adjacent to the seawater feed stream, many particles in the seawater could be trapped in the support layer. Considering these factors, the AL-FS mode is suitable for the DSARO process.

To analyze the concentration polarization effect in more detail, the draw solution concentration is fixed at 30 g/l, and the amount of effective osmotic pressure difference and the concentrations at the surface of membrane are shown in Fig. 6. In Figs. 6 (a) and (c), the effective osmotic pressure difference ($\pi_{F,m}$-$\pi_{D,m}$), the effective osmotic pressure difference with no ICP ($\pi_{F,b}$-$\pi_{D,m}$ in AL-FS and $\pi_{F,m}$-$\pi_{D,b}$ in AL-DS mode), and the bulk osmotic pressure difference ($\pi_{F,b}$-$\pi_{D,b}$) are shown. The ICP, rather than the ECP, appearance accounts for a large percentage of the effective osmotic pressure increase. As can be seen in Figs. 6 (b) and (d), the ICP effect is reduced by decreasing the membrane structure parameter. Even if the best available PRO membrane technology could be utilized in the DSARO process, the impact of the ICP effect remains high. It is therefore seen that membranes with a smaller structure parameter should be developed to decrease the required applied pressure in the 1st RO process more significantly. However, in state-of-the-art membrane technology, the applied pressure in the 1st RO process could be considerably reduced, and will be discussed in the following sections.

Table 4 shows the membrane parameters and maximum endurable pressure in PRO membranes from recent literature. As the PRO operation is the most similar to the DSARO process in terms of pressure application and utilization of draw solution, the membrane development status in the PRO process can be a barometer for the applicability in the DSARO process. The S parameter has decreased by approximately 0.13 mm, and the maximum endurable pressure of the membrane is reported as 27.6 bar [47]. Thus, in this study, this membrane is assumed as the best available technology in the PRO process, and the membrane characteristics are used as the base simulation conditions in the following sections.

3.2. Energy consumptions and applied pressures in the DSARO process

As mentioned in Section 2.5, the independent and important variables were already selected. In this section, default values of the independent variables were fixed at 30 g/l for C_{draw}, 1 for Q_{draw}/Q_{feed}, and 1.3×10^{-4} m for S. By changing these variables, the effect of these variables on the applied pressures and specific energy consumption in the DSARO process can be calculated.

3.2.1. Effect of draw solution concentration (C_{draw})

As shown in Fig. 7, increasing the draw solution concentration decreases the pressure requirement in the 1st RO process, while increasing that of the 2nd RO process. When increasing rec_{1st} from 40% to 45%, the applied pressure in the 1st RO process increases by approximately 5 bar. On the other hand, the pressure requirements in the 2nd RO process are almost the same, so the lines representing applied pressure in the 2nd RO process in Fig. 7 (a) overlap. At 30 g/l of draw solution concentration, the applied pressures in the 1st RO process are approximately 40 bar with 45% recovery, and 36 bar with 40% recovery. In the 2nd RO process, approximately 30 bar pressure is required for both the 45% and 40% recoveries. Thus, the DSARO process can be operated under 40 bar condition when the draw solution concentration is 30 g/l and rec_{1st} is 40%. The importance of this condition will be

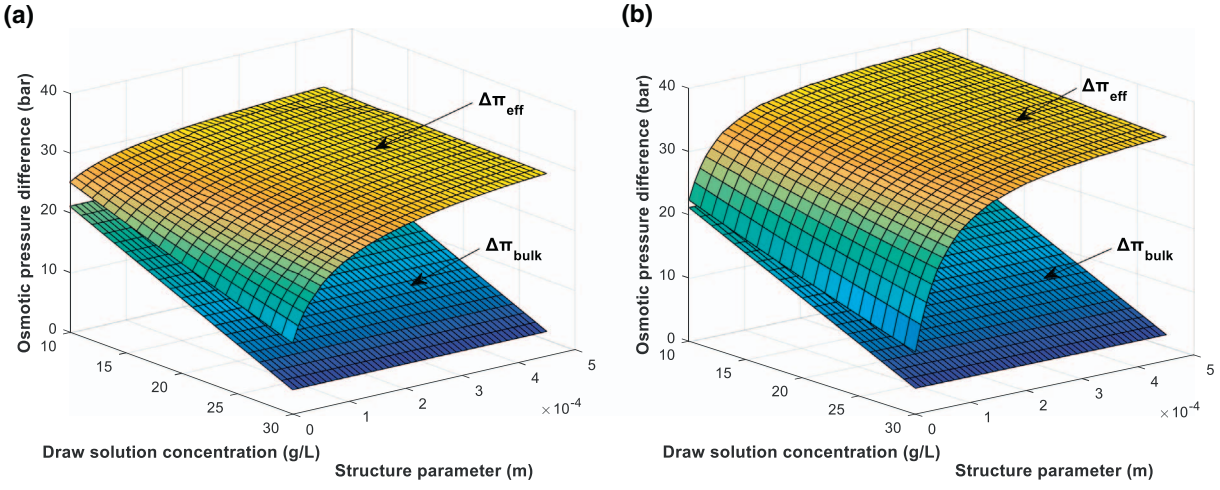

Fig. 5. Bulk and effective osmotic pressure differences when changing the concentration of draw solution and membrane structure parameter in the 1st RO module: (a) AL-FS mode, and (b) AL-DS mode.

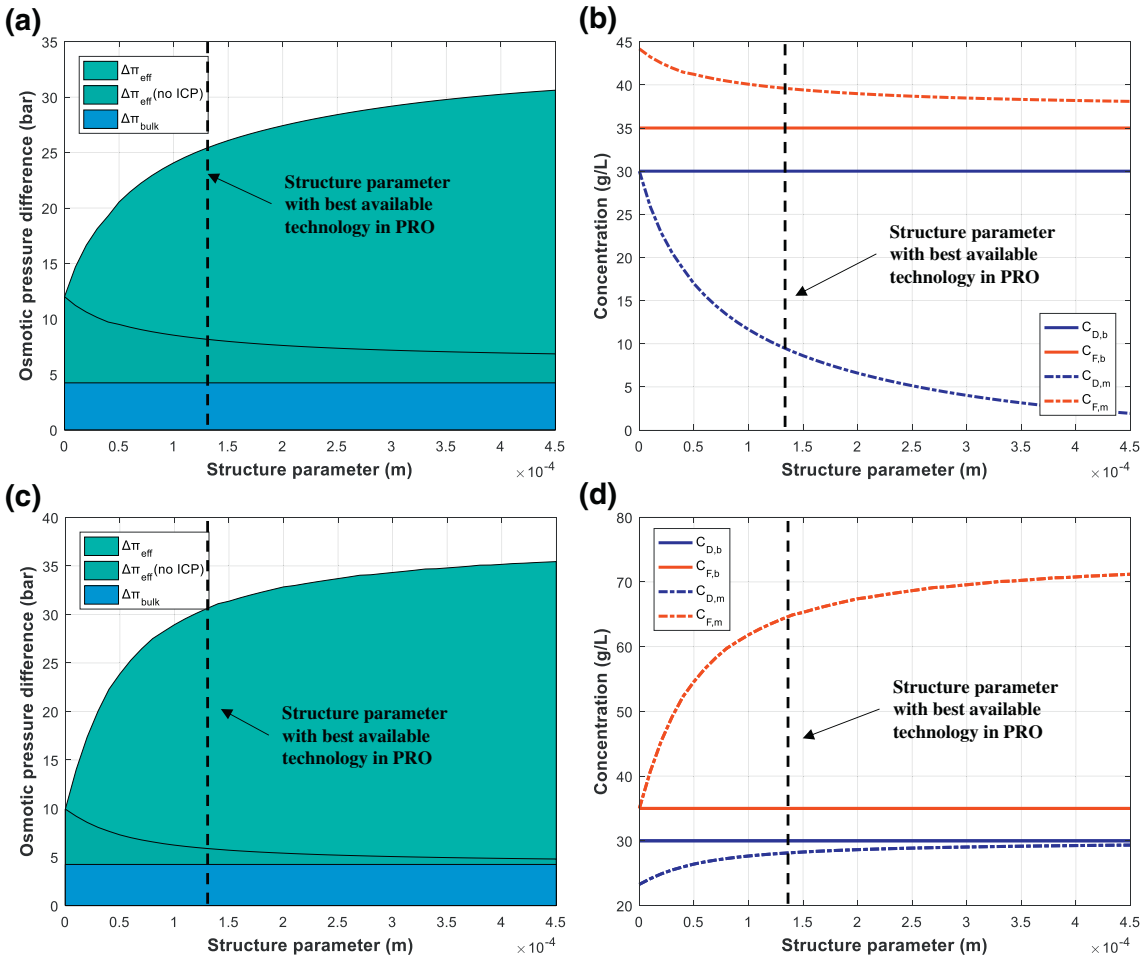

Fig. 6. Effects of ICP and ECP appearances on osmotic pressure differences and concentrations at different membrane structure parameters: (a) bulk and effective osmotic pressure differences in the AL-FS mode, (b) bulk and membrane surface concentrations in the AL-FS mode, (c) bulk and effective osmotic pressure differences in the AL-DS mode, and (d) bulk and membrane surface concentrations in the AL-DS mode.

Table 4
Comparison of the characteristics of PRO membranes.

Membrane type	A value (m/(Pa·s))	S value (mm)	Max P (bar)	Reference
HTI-TFC	6.92×10^{-12}	0.564	48	[48]
TNC	3.42×10^{-12}	0.149	15.2	[49]
TNC	1.06×10^{-11}	0.135	15.2	[49]
TFC	9.22×10^{-12}	0.460	9	[50]
PEI-TFC	7.22×10^{-12}	0.476	25	[51]
PES-TFC	9.17×10^{-12}	0.450	21	[52]
TE-TFC	1.16×10^{-12}	0.133	27.6	[47]
pTFC	1.47×10^{-11}	0.307	11.5	[53]
mTFC	7.86×10^{-12}	0.273	11.5	[53]

discussed in later.

Specific energy consumption is also changed by the draw solution concentration. Since the applied pressures are changed in both the 1st and 2nd RO processes, specific energy consumptions in each process change with the same trends. The overall SEC increases slightly with increasing draw solution concentration. Therefore, as the draw solution concentration increases, the overall SEC increases slightly, but the pressure in the 1st RO process could be reduced.

3.2.2. Effect of flow rate ratio (Q_{draw}/Q_{feed})

A smaller flow rate ratio implies that the draw solution concentration in the 1st RO module would change more significantly, compared to a larger flow rate ratio at the same 1st RO recovery, and it makes the applied pressure in the 1st RO process increase to obtain the required 1st RO recovery. Despite this disadvantage, a lower concentration of the effluent draw solution from the 1st RO process has lower osmotic pressure, which might reduce the pressure requirement in the 2nd RO process. In addition, the smaller flow rate could reduce the energy requirement in the high-pressure pump. However, it should be considered that the recovery of the 2nd RO process should be higher to obtain the same amount of water permeated in the 1st RO process. The higher recovery might increase the applied pressure in the 2nd RO process. In other words, these factors are all coupled and adversely affect the applied pressure. Therefore, the simulation should be carried out to identify how the overall results of applied pressure and specific energy consumption would be changed.

As shown in Fig. 8, the applied pressure in the 1st RO process decreases; however, after a certain point, increases slightly as the flow rate ratio increases, due to a higher pressure drop in the 1st RO module with the higher draw solution velocity. Thus, there is a minimum point of flow rate ratio between 0.8 and 1.0. The applied pressure in the 2nd RO process stays approximately the same regardless of the flow rate ratio. As mentioned above paragraph, the counter-affecting factors lead to the almost same pressures in the 2nd RO process.

The SEC graph shows that a higher flow rate ratio increases overall SEC regardless of the 1st RO recovery. However, considering that a lower flow rate ratio results in considerably higher applied pressure in the 1st RO process, a flow rate ratio of approximately 0.8 would be appropriate.

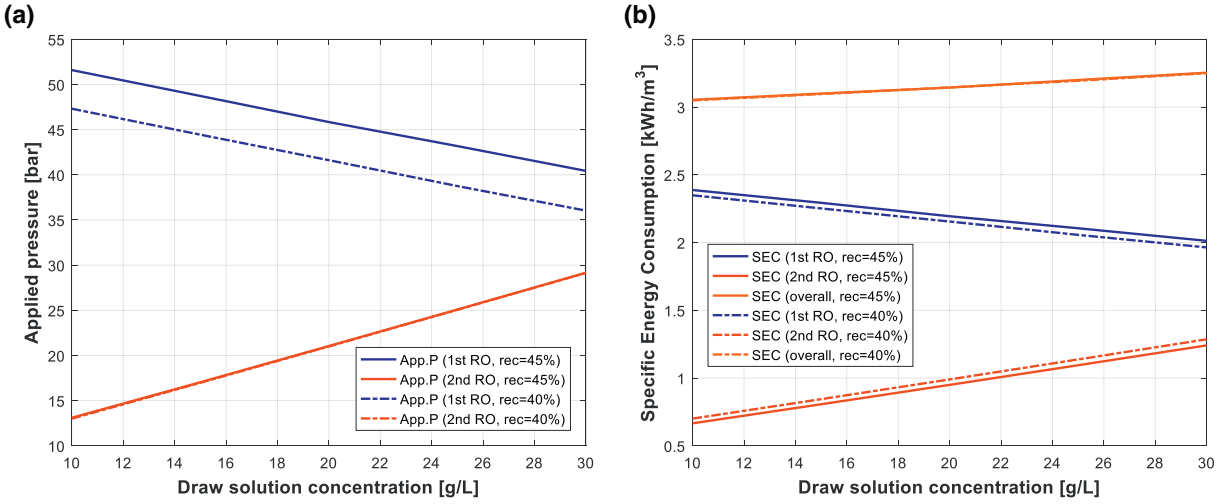

Fig. 7. Effects of draw solution concentration on (a) applied pressures, and (b) specific energy consumptions, of each RO stage in the DSARO process.

3.2.3. *Effect of membrane structure parameter (S)*

A smaller membrane structure parameter can reduce the effect of ICP, but, if it is too low, the membrane would not withstand the high applied pressure. This simulation analysis will determine how much the applied pressure should be resisted with different membrane structure parameters to operate the DSARO process for a seawater desalination system.

As the structure parameter decreases, a lowered ICP effect could reduce the required pressure in the 1st RO process. The structure parameter should decrease below 0.12 mm to obtain less than 40 bar of pressure in the 1st RO process with a 45% recovery. Even considering state-of-the-art membrane technology, this type of membrane, which is very thin and strong, cannot be easily manufactured. However, by decreasing the 1st RO recovery, the pressure load on the membrane could be reduced. Even though the latest available technology in PRO membranes cannot yet meet the pressure requirements of the DSARO process, the process could become feasible when this technology does arrive. In such cases, the analysis of this section could be utilized.

The SEC graph in Fig. 9 (b) shows that the energy efficiency would be enhanced if a thinner membrane were available. With a membrane structure parameter of 0.13 mm, the overall SEC is 3.25 kWh/m^3.

3.2.4. *Comparison with the conventional RO process*

To compare the applied pressure and SEC of the DSARO process with those of the conventional RO process, an RO process simulation was conducted for the same conditions. As shown in Fig. 10, the applied pressure in the conventional RO process is approximately 60–65 bar, and the SEC 2.55–2.63 kWh/m^3. Even though the SEC of the conventional RO process is lower than that of the DSARO process, the pressure requirement is more than 20 bar higher. The main reasons why the energy consumption of the DSARO process is higher than the conventional RO process are ICP appearance in the 1st RO module and two times of ECP appearance, as opposed to once in the conventional RO process. In addition, the draw solution circulating pump in the DSARO process requires electricity. Because of this, the energy efficiency of the DSARO process is lower, but it can be operated in a lower pressure range than the conventional RO process. Therefore, the installation cost and membrane replacement cost of the DSARO process would be lower than that of the conventional RO process, but the cost of electricity would be greater. The detailed analysis will be conducted in a later section.

Fresh water quality is also important factor to confirm whether the proposed process is feasible or not for desalination. Even though the BWRO membrane which has higher salt permeability than the SWRO membrane is utilized in 2nd RO process, the fresh water quality in the DSARO process is shown as 300–370 ppm by changing recovery from 40% to 45%. The conventional RO process shows 200–300 ppm of water quality. Since water which contains total dissolved solids less

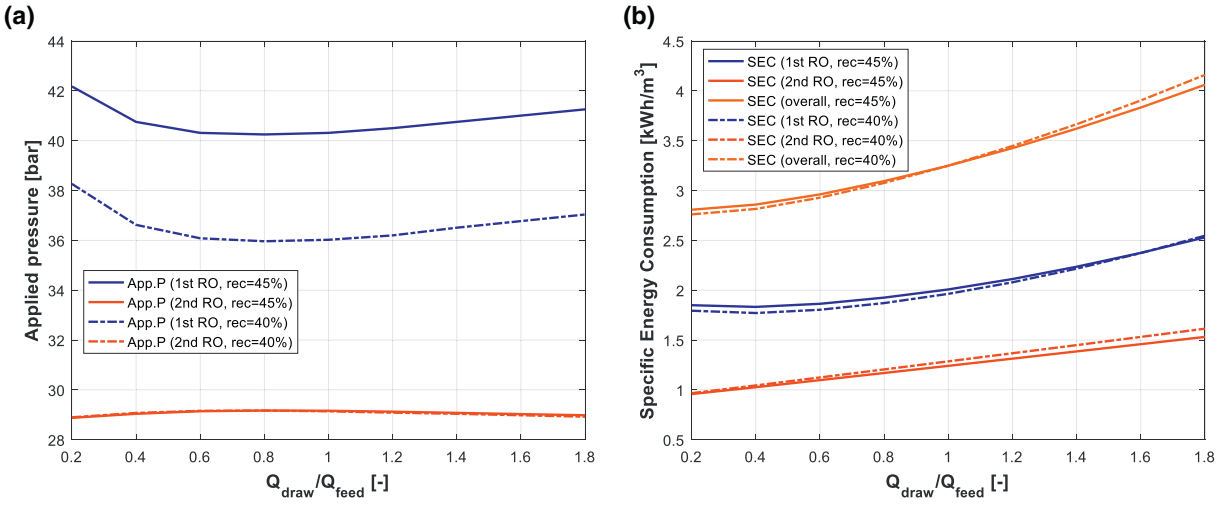

Fig. 8. Effects of flow rate ratio on (a) applied pressures, and (b) specific energy consumptions, of each RO stage in the DSARO process.

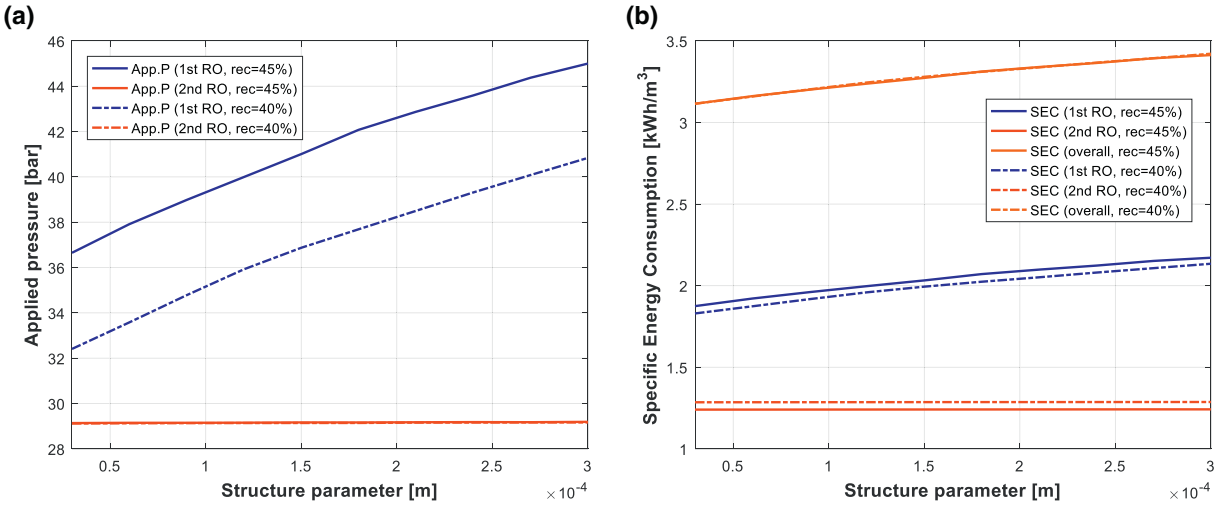

Fig. 9. Effects of membrane structure parameter on (a) applied pressures, and (b) specific energy consumption, of each RO stage in the DSARO process.

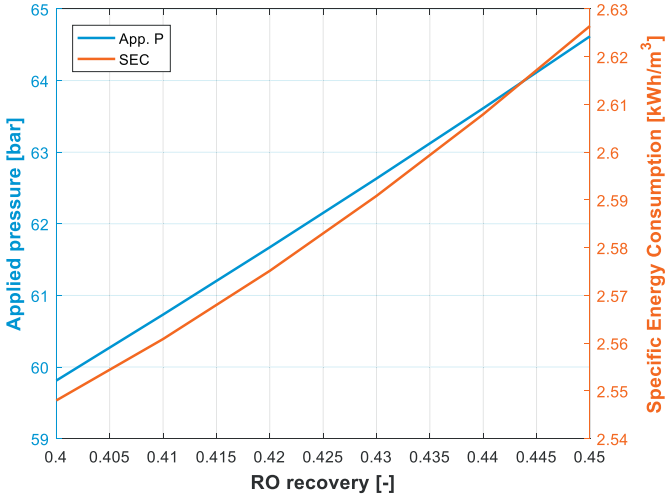

Fig. 10. Applied pressure and specific energy consumption in the conventional RO process by changing RO recovery.

than 500 ppm is classified as fresh water, the DSARO process is suitable for desalination.

3.3. Cost estimation and sensitivity analysis for feasibility study of the DSARO process

With the developed cost estimation model above, cost estimation was carried out to compare the DSARO process with the conventional RO process. In this study, the capital cost of the DSARO process is assumed as the sum of the costs of two BWRO processes in sequence, as the operating pressure of the DSARO is similar to that of the BWRO [43]. The cost breakdown data and SWC are listed in Table 5. The cost variation in the cost of electricity is due to the RO recovery change from 40% to 45%. A fixed TAC in the DSARO process is because the SEC of the DSARO process is almost same within the overall recovery range (40–45%). Even though each cost estimation result would contain statistical errors, the relative cost comparison could be significantly unaffected by statistical errors by using same basis for cost estimation. Thus, the relative cost comparison is utilized for cost-based feasibility study.

Compared to the conventional RO process, the DSARO process has a 10% lower SWC. In more detail, the DSARO process has a 13% lower CAPEX and a 7% lower OPEX than the conventional RO process. Even

Table 5
Cost breakdown data of DSARO and conventional RO processes with recovery (40–45%).

	DSARO process	Conventional RO process
CAPEX		
Direct capital cost		
EPC cost	$ 14,071,477	$ 16,135,191
Indirect capital cost		
Freight & insurance rate during construction	$ 703,574	$ 806,760
Owner's cost rate	$ 1,069,432	$ 1,226,275
Contingency rate	$ 1,407,148	$ 1,613,519
Construction overhead	$ 1,722,349	$ 1,974,947
OPEX		
Cost of electricity	$ 854,098	$ 669,613–$ 690,227
Membrane replacement cost	$ 197,001	$ 451,785
Spare parts replacement and insurance cost	$ 281,430	$ 322,704
Chemical cost of product water	$ 82,125	$ 82,125
Labor cost	$ 164,250	$ 164,250
Annualized cost		
TACC	$ 1,654,238	$ 1,896,848
TAC	$ 3,233,141	$ 3,587,325–$ 3,607,939
SWC	$ 0.984	$ 1.092–$ 1.098

though the electricity cost of the DSARO process is 27% higher than that of the conventional RO process, the larger amount of membrane replacement cost saving compensates for this. The reduction in the SWC of the DSARO process is mostly based on the lower operating pressure, which was assumed to be in the pressure range of the BWRO process.

However, the cost estimation method is based on the ratios of EPC cost and membrane capital cost in Eqns. (24) and (27). If the cost ratios in the actual DSARO process were changed, the SWC of the DSARO process would be changed. A sensitivity analysis was performed by changing the EPC cost ratio between the DSARO and the BWRO processes and changing the membrane replacement cost ratio from 0.1 (BWRO) to 0.2 (SWRO) to determine the impact of the cost ratios on the SWC. The default values were 2 for the EPC cost ratio and 0.1 for the membrane replacement cost ratio in the above cost estimation.

As shown in Fig. 11, the sensitivity analysis reveals how much the SWC could be affected by each cost ratio. As the EPC cost ratio increases while fixing the membrane replacement cost ratio as 0.1, the SWC of the DSARO process becomes higher, and is more than the conventional RO process cost if the EPC cost ratio was higher than 2.35. When the membrane replacement cost ratio increases from 0.1 to 0.2 with a fixed

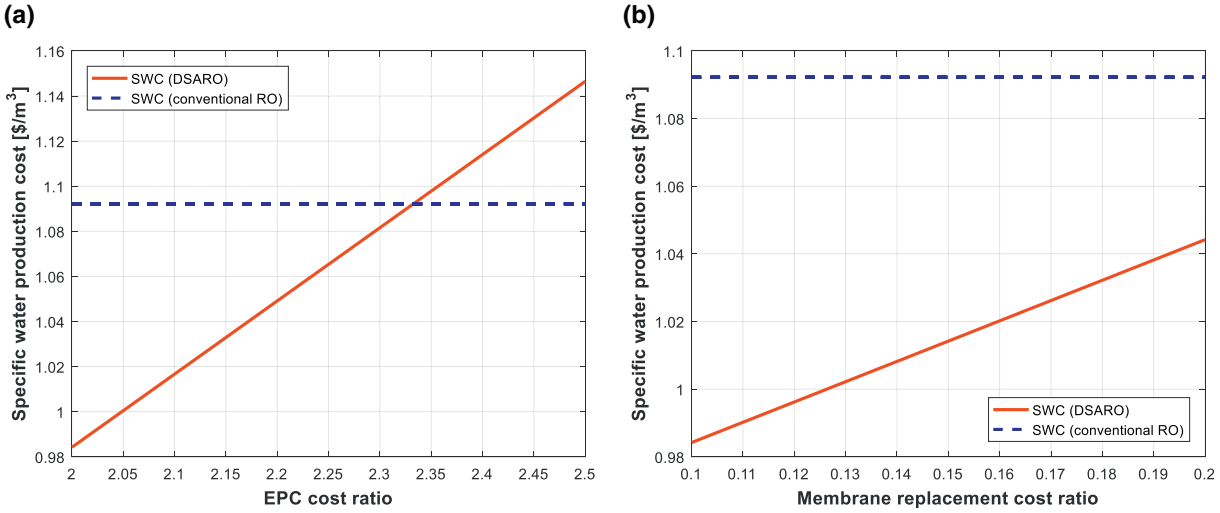

Fig. 11. Sensitivity analysis on the (a) EPC cost ratio and (b) membrane replacement cost ratio related to the specific water production cost of the DSARO process.

EPC cost ratio of 2, the cost saving compared to the conventional RO process drops from 10% to 5%, which is still lower than the SWC of the conventional RO process. Thus, the EPC cost ratio has a higher impact on the SWC of the DSARO process.

3.4. Required conditions for the DSARO process feasible

The most important factor in efficiently utilizing the DSARO process is the operating pressure in the 1st and 2nd RO processes. If the operating pressure is greater than the pressure range of the BWRO process, the EPC cost would increase significantly and the economic feasibility of the DSARO process would be weakened. Even though the maximum operating pressure in the BWRO process has been reported as 41 bar [43], an operating pressure no greater than 35 bar would be a reasonable pressure condition. In the above results, the DSARO process can be operated at approximately 35 bar in the 1st RO process and 30 bar in the 2nd RO process, with 40% overall recovery. Even though the overall recovery is slightly lower than the conventional RO process, the increase in recovery raises the pressure requirement in the 1st RO process up to 41 bar, which is not suitable to effectively operate the DSARO process. Therefore, the best conditions of the DSARO process for economic feasibility would be approximately 40% recovery and 35 bar.

Additionally, a thin and strong membrane should be developed. With the current best available membrane technology, a membrane with a 0.133 mm structure parameter and a maximum pressure of 27.6 bar has been reported. The membrane structure parameter is enough to drive the DSARO process as analyzed above, but the maximum operating pressure is lower than the required pressure value (35 bar). Thus, if the membrane could withstand more than 35 bar, and its price be reasonable, the membrane could be utilized in the DSARO process. If these conditions were satisfied, the SWC of the DSARO process would become 10% lower than that of the conventional RO process, and it would be a cost-efficient alternative method for seawater desalination.

4. Conclusions

This study proposes a new process, named draw solution assisted reverse osmosis (DSARO) process. The DSARO process utilizes a draw solution not to induce spontaneous water molecules transfer by high concentration draw solution, but to decrease osmotic pressure difference by low concentration draw solution. Thus, the DSARO process can decrease the high-pressure requirement in the conventional RO process by utilizing a two-stage low-pressure RO process. A mathematical model and cost estimation model were developed to determine the amount of water permeation and required pressure in the DSARO process. The results showed that even though the applied pressure is higher than the bulk osmotic pressure difference due to concentration polarization, it could be reduced to approximately 35 bar in the 1st RO process and 30 bar in the 2nd RO process. Although the specific energy consumption is higher than the conventional RO process, the cost estimation results revealed that the specific water production cost of the DSARO process is 10% lower than that of the conventional RO process. The sensitivity analysis showed that the EPC cost ratio is the most critical factor in terms of economic feasibility of the DSARO process, and it could be a more cost-effective technology in seawater desalination if the EPC cost ratio was lower than 2.35. The DSARO process could be feasible if the membrane had a structure parameter lower than 0.13 mm, and a maximum operating pressure higher than 35 bar. Considering the best available membrane technology, the DSARO process could be realized commercially in the near future.

Acknowledgements

This work is supported by the Korea Agency for Infrastructure Technology Advancement (KAIA) grant funded by the Ministry of Land, Infrastructure and Transport (Grant 17IFIP-B116952-02), and Korea University.

References

[1] T.Y. Cath, A.E. Childress, M. Elimelech, Forward osmosis: principles, applications, and recent developments, J. Membr. Sci. 281 (2006) 70–87.
[2] T.-S. Chung, S. Zhang, K.Y. Wang, J. Su, M.M. Ling, Forward osmosis processes: yesterday, today and tomorrow, Desalination 287 (2012) 78–81.
[3] N.M. Mazlan, D. Peshev, A.G. Livingston, Energy consumption for desalination—a comparison of forward osmosis with reverse osmosis, and the potential for perfect membranes, Desalination 377 (2016) 138–151.
[4] R.K. McGovern, On the potential of forward osmosis to energetically outperform reverse osmosis desalination, J. Membr. Sci. 469 (2014) 245–250.
[5] D.L. Shaffer, J.R. Werber, H. Jaramillo, S. Lin, M. Elimelech, Forward osmosis: where are we now? Desalination 356 (2015) 271–284.
[6] M. Xie, L.D. Nghiem, W.E. Price, M. Elimelech, A forward osmosis–membrane distillation hybrid process for direct sewer mining: system performance and limitations, Environ. Sci. Technol. 47 (2013) 13486–13493.
[7] B.D. Coday, P. Xu, E.G. Beaudry, J. Herron, K. Lampi, N.T. Hancock, T.Y. Cath, The sweet spot of forward osmosis: treatment of produced water, drilling wastewater, and other complex and difficult liquid streams, Desalination 333 (2014) 23–35.
[8] L.A. Hoover, W.A. Phillip, A. Tiraferri, N.Y. Yip, M. Elimelech, Forward with osmosis: emerging applications for greater sustainability, Environ. Sci. Technol. 45 (2011) 9824–9830.
[9] R.V. Linares, Z. Li, S. Sarp, S.S. Bucs, G. Amy, J.S. Vrouwenvelder, Forward osmosis niches in seawater desalination and wastewater reuse, Water Res. 66 (2014) 122–139.
[10] A. Altaee, G. Zaragoza, H.R. van Tonningen, Comparison between forward osmosis-reverse osmosis and reverse osmosis processes for seawater desalination,

Desalination 336 (2014) 50–57.
[11] R.V. Linares, Z. Li, V. Yangali-Quintanilla, N. Ghaffour, G. Amy, T. Leiknes, J. Vrouwenvelder, Life cycle cost of a hybrid forward osmosis–low pressure reverse osmosis system for seawater desalination and wastewater recovery, Water Res. 88 (2016) 225–234.
[12] V. Yangali-Quintanilla, Z. Li, R. Valladares, Q. Li, G. Amy, Indirect desalination of Red Sea water with forward osmosis and low pressure reverse osmosis for water reuse, Desalination 280 (2011) 160–166.
[13] D.Y. Kim, B. Gu, J.H. Kim, D.R. Yang, Theoretical analysis of a seawater desalination process integrating forward osmosis, crystallization, and reverse osmosis, J. Membr. Sci. 444 (2013) 440–448.
[14] T.N. Bitaw, K. Park, D.R. Yang, Optimization on a new hybrid forward osmosis-electrodialysis-reverse osmosis seawater desalination process, Desalination 398 (2016) 265–281.
[15] L. Chekli, S. Phuntsho, J.E. Kim, J. Kim, J.Y. Choi, J.-S. Choi, S. Kim, J.H. Kim, S. Hong, J. Sohn, A comprehensive review of hybrid forward osmosis systems: performance, applications and future prospects, J. Membr. Sci. 497 (2016) 430–449.
[16] T.-S. Chung, X. Li, R.C. Ong, Q. Ge, H. Wang, G. Han, Emerging forward osmosis (FO) technologies and challenges ahead for clean water and clean energy applications, Curr. Opin. Chem. Eng. 1 (2012) 246–257.
[17] A. Altaee, G. Zaragoza, A conceptual design of low fouling and high recovery FO–MSF desalination plant, Desalination 343 (2014) 2–7.
[18] P.H. Duong, T.-S. Chung, Application of thin film composite membranes with forward osmosis technology for the separation of emulsified oil–water, J. Membr. Sci. 452 (2014) 117–126.
[19] Y. Cui, Q. Ge, X.-Y. Liu, T.-S. Chung, Novel forward osmosis process to effectively remove heavy metal ions, J. Membr. Sci. 467 (2014) 188–194.
[20] S. Phuntsho, H.K. Shon, S. Hong, S. Lee, S. Vigneswaran, A novel low energy fertilizer driven forward osmosis desalination for direct fertigation: evaluating the performance of fertilizer draw solutions, J. Membr. Sci. 375 (2011) 172–181.
[21] K. Park, D.Y. Kim, D.R. Yang, Theoretical analysis and economic evaluation of draw solution assisted reverse osmosis process, Computing and Systems Technology Division 2015 - Core Programming Area at the 2015 AIChE Annual Meeting, 2015, pp. 112–120.
[22] K. Park, D.Y. Kim, D.R. Yang, Cost-based analysis about a newly designed two-staged reverse osmosis process with draw solute, 26th European Symposium on Computer Aided Process Engineering: Part A and B, Elsevier, 2016, p. 223.
[23] B. Gu, D. Kim, J. Kim, D.R. Yang, Mathematical model of flat sheet membrane modules for FO process: plate-and-frame module and spiral-wound module, J. Membr. Sci. 379 (2011) 403–415.
[24] D.Y. Kim, B. Gu, D.R. Yang, An explicit solution of the mathematical model for osmotic desalination process, Korean J. Chem. Eng. 30 (2013) 1691–1699.
[25] S.S. Hong, W. Ryoo, M.-S. Chun, G.-Y. Chung, Effects of membrane characteristics on performances of pressure retarded osmosis power system, Korean J. Chem. Eng. 32 (2015) 1249–1257.
[26] J.R. McCutcheon, M. Elimelech, Influence of concentrative and dilutive internal concentration polarization on flux behavior in forward osmosis, J. Membr. Sci. 284 (2006) 237–247.
[27] K. Lee, R. Baker, H. Lonsdale, Membranes for power generation by pressure-retarded osmosis, J. Membr. Sci. 8 (1981) 141–171.
[28] Y. Xu, X. Peng, C.Y. Tang, Q.S. Fu, S. Nie, Effect of draw solution concentration and operating conditions on forward osmosis and pressure retarded osmosis performance in a spiral wound module, J. Membr. Sci. 348 (2010) 298–309.
[29] C. Bae, K. Park, H. Heo, D.R. Yang, Quantitative estimation of internal concentration polarization in a spiral wound forward osmosis membrane module compared to a flat sheet membrane module, Korean J. Chem. Eng. 34 (2017) 844–853.
[30] W. Zhou, L. Song, T.K. Guan, A numerical study on concentration polarization and system performance of spiral wound RO membrane modules, J. Membr. Sci. 271 (2006) 38–46.
[31] A. Malek, M. Hawlader, J. Ho, Design and economics of RO seawater desalination, Desalination 105 (1996) 245–261.
[32] M.G. Marcovecchio, P.A. Aguirre, N.J. Scenna, Global optimal design of reverse osmosis networks for seawater desalination: modeling and algorithm, Desalination 184 (2005) 259–271.
[33] N. Ghaffour, T.M. Missimer, G.L. Amy, Technical review and evaluation of the economics of water desalination: current and future challenges for better water supply sustainability, Desalination 309 (2013) 197–207.
[34] S. Loutatidou, B. Chalermthai, P.R. Marpu, H.A. Arafat, Capital cost estimation of RO plants: GCC countries versus southern Europe, Desalination 347 (2014) 103–111.
[35] H.M. Ettouney, H.T. El-Dessouky, R.S. Faibish, P.J. Gowin, Evaluating the economics of desalination, Chem. Eng. Prog. 98 (2002) 32–39.
[36] S. Loutatidou, H.A. Arafat, Techno-economic analysis of MED and RO desalination powered by low-enthalpy geothermal energy, Desalination 365 (2015) 277–292.
[37] L.F. Greenlee, D.F. Lawler, B.D. Freeman, B. Marrot, P. Moulin, Reverse osmosis desalination: water sources, technology, and today's challenges, Water Res. 43 (2009) 2317–2348.
[38] A. Ruiz-García, E. Ruiz-Saavedra, 80,000 h operational experience and performance analysis of a brackish water reverse osmosis desalination plant. Assessment of membrane replacement cost, Desalination 375 (2015) 81–88.
[39] V. Geraldes, N.E. Pereira, M. Norberta de Pinho, Simulation and optimization of medium-sized seawater reverse osmosis processes with spiral-wound modules, Ind. Eng. Chem. Res. 44 (2005) 1897–1905.
[40] J. Andrianne, F. Alardin, Thermal and membrane process economics: optimized selection for seawater desalination, Desalination 153 (2003) 305–311.
[41] A. Ghobeity, A. Mitsos, Optimal time-dependent operation of seawater reverse osmosis, Desalination 263 (2010) 76–88.
[42] S. Loutatidou, N. Liosis, R. Pohl, T.B. Ouarda, H.A. Arafat, Wind-powered desalination for strategic water storage: techno-economic assessment of concept, Desalination 408 (2017) 36–51.
[43] Y.-Y. Lu, Y.-D. Hu, X.-L. Zhang, L.-Y. Wu, Q.-Z. Liu, Optimum design of reverse osmosis system under different feed concentration and product specification, J. Membr. Sci. 287 (2007) 219–229.
[44] B. Peñate, L. García-Rodríguez, Current trends and future prospects in the design of seawater reverse osmosis desalination technology, Desalination 284 (2012) 1–8.
[45] K.M. Sassi, I.M. Mujtaba, MINLP based superstructure optimization for boron removal during desalination by reverse osmosis, J. Membr. Sci. 440 (2013) 29–39.
[46] A. Abbas, Simulation and analysis of an industrial water desalination plant, Chem. Eng. Process. 44 (2005) 999–1004.
[47] S.S. Manickam, J.R. McCutcheon, Model thin film composite membranes for forward osmosis: demonstrating the inaccuracy of existing structural parameter models, J. Membr. Sci. 483 (2015) 70–74.
[48] A.P. Straub, N.Y. Yip, M. Elimelech, Raising the bar: increased hydraulic pressure allows unprecedented high power densities in pressure-retarded osmosis, Environ. Sci. Tech. Let. 1 (2013) 55–59.
[49] X. Song, Z. Liu, D.D. Sun, Energy recovery from concentrated seawater brine by thin-film nanofiber composite pressure retarded osmosis membranes with high power density, Energy Environ. Sci. 6 (2013) 1199–1210.
[50] S. Chou, R. Wang, L. Shi, Q. She, C. Tang, A.G. Fane, Thin-film composite hollow fiber membranes for pressure retarded osmosis (PRO) process with high power density, J. Membr. Sci. 389 (2012) 25–33.
[51] M. Tian, R. Wang, K. Goh, Y. Liao, A.G. Fane, Synthesis and characterization of high-performance novel thin film nanocomposite PRO membranes with tiered nanofiber support reinforced by functionalized carbon nanotubes, J. Membr. Sci. 486 (2015) 151–160.
[52] S. Zhang, P. Sukitpaneenit, T.-S. Chung, Design of robust hollow fiber membranes with high power density for osmotic energy production, Chem. Eng. J. 241 (2014) 457–465.
[53] N.-N. Bui, J.R. McCutcheon, Nanofiber supported thin-film composite membrane for pressure-retarded osmosis, Environ. Sci. Technol. 48 (2014) 4129–4136.